A direct method to determine the degree of crystallinity and lamellar thickness of polymers: application to polyethylene*

Anthony J. Ryan†
Manchester Materials Science Centre, UMIST, Grosvenor Street, Manchester M1 7HS, UK

and Wim Bras‡, Geoffrey R. Mant and Gareth E. Derbyshire
SERC Daresbury Laboratory, Warrington WA4 4AD, UK

Time-resolved small-angle X-ray scattering (SAXS) and wide-angle X-ray scattering (WAXS) patterns have been simultaneously obtained during melting and crystallization of high-density polyethylene using a newly constructed camera at the SRS, Daresbury. The data have been analysed to yield the long spacing, the degree of crystallinity and the lamellar thickness in the context of the two-phase model. The long spacing was obtained from the peak in the Lorentz-corrected SAXS pattern. The degree of crystallinity was obtained from a combination of the SAXS invariant and the integrated WAXS intensity of the crystals. The invariant passes through a maximum at 50% crystallinity and the integrated WAXS intensity is a minimum for the melt. Thus two points in the linear relationship between the WAXS intensity and the degree of crystallinity are known, affording calibration. Calculation of the degree of crystallinity by solving the quadratic in the SAXS invariant gave good agreement with the WAXS result. The long spacing and the degree of crystallinity may be combined in the two-phase model to estimate the lamellar thickness, an important parameter in determining mechanical properties.

(Keywords: degree of crystallinity; lamellar thickness; polyethylene)

INTRODUCTION

The degree of crystallinity, defined as either the weight or volume fraction of the crystalline phase of a semicrystalline polymer, is of fundamental importance in defining the physical and chemical properties of the polymer. Several methods have been developed to evaluate this important parameter[2], including density measurement (density column), differential scanning calorimetry (d.s.c.) and differential thermal analysis (d.t.a.), spectroscopic techniques (n.m.r., *FT*i.r. and Raman) and the X-ray techniques of wide-angle and small-angle scattering (WASX and SAXS)[3]. Each of these methods is based on a different physical feature and uses a different definition of crystalline order. This fact accounts for the differences reported by the various methods. Some of these techniques inevitably rely on calibration with wholly crystalline and/or wholly amorphous standards, and furthermore these techniques are generally limited to making single-point measurements on stable systems; this is especially true about the density column technique.

Crystallization kinetics are also of immense technical importance[1,2]. The process of crystallization is the primary solidification mechanism for over half of the polymeric artefacts currently produced. The earliest methods for studying the kinetics of crystallization involved measurements of volume change. In order to study crystallization kinetics by this technique an isothermal bath is essential, as the only change in volume must be that associated with the crystallization process. Isothermal d.s.c. is another method of studying crystallization kinetics by measuring the enthalpy of crystallization[1]. Both of these techniques have reasonable time resolution (with automation ~ 1 s) but are limited to isothermal situations. The d.s.c. technique can be used for non-isothermal crystallization but the analysis has many assumptions and is computationally intense[4].

The radial growth rate of polymer spherulites may be studied by optical microscopy[2]. Unlike the overall rate of crystallization, which is dominated by the nucleation process, the radial growth rate v is a function only of the degree of undercooling and the molecular weight for a given polymer. In spherulites, the commonest form of melt-crystallized polymer, the chain axis is perpendicular to the radius. Thus the growth situation is simplified to being one-dimensional, and the lateral growth is generally observed to be linear with time. The growth process is a property of the polymer and is dependent on the supercooling and molecular weight but not on the nucleation mechanism, and v passes through a maximum between T_g and T_m. For example, the change in linear dimensions of polyoxyethylene lamellae crystallized from solution follows the same linear equation as the growth of spherulites in heavily nucleated polypropylene. The temperature dependence of v is easy to interpret qualitatively – it is a complex product of the driving force

* Presented at 'The Polymer Conference', 20–22 July 1993, University of Cambridge, UK
† To whom correspondence should be addressed
‡ Current address: NWO, The Hague, The Netherlands

0032-3861/94/21/4537-08

for crystallization and the mobility of the system. As the temperature is reduced from the thermodynamic melting point T_m^0, the driving force for crystallization ε increases as it is directly proportional to the supercooling ($\varepsilon \approx T_m^0 - T$). The mobility of the system decreases asymptotically as the glass transition temperature is approached because the mobility is the reciprocal of the viscosity, i.e. $\eta \approx 1/(T - T_g)$. The optical microscopy technique is, therefore, very useful in looking at the isothermal growth of lamellae and spherulites and, at best, has the time resolution of video.

The spectroscopic techniques provide lots of extra information about the local environment of chain segments. Time resolution is possible with these techniques[5] but this is limited by the specific instruments and their counting statistics; for example, the fast spectra acquisition time for *FT*i.r. is ~ 1 s. However, the spectroscopic techniques have advantages over the more conventional techniques in that non-isothermal experiments may be conducted.

The technique of wide-angle X-ray scattering (WAXS) may be used to solve the crystal structure (establish the unit cell and atomic positions) if the full diffraction pattern of a single crystal or fibre is available[3,6]. Owing to the polycrystalline nature of most polymers, it is more common to obtain the one-dimensional diffraction pattern and, wherever possible, index the structure from this. There are several different procedures[3] used to derive the degree of crystallinity from WAXS which fall into two broad classes:

1. procedures deriving the relative degrees of crystallinity by means of crystalline and amorphous standards[7–9]; and
2. procedures evaluating the absolute degree of crystallinity based on a proper understanding of the diffuse scattering and the ratio of the integrated intensity under the crystalline peaks to the integrated intensity under the complete scattering pattern[10–13].

The majority of the methods for determining the degree of crystallinity from WAXS rely on the arbitrary separation of the amorphous scattering; however, there are some techniques that use a simulation of the scattering curve which get round this problem[11,13].

Small-angle X-ray scattering (SAXS) is a well-established technique for studying the morphology of multiphase polymers[3]. X-Rays are scattered by regions with different electron densities. It is often used in tandem with d.s.c. to study polymer crystallization and microphase separation in block copolymers. Information is obtained in the form of a scattering pattern; as with WAXS, unoriented materials have one-dimensional patterns which can be analysed using Bragg's law to give information on structural features with size scales from 50 to 1000 Å (1 Å = 0.1 nm) – for liquid crystalline and semicrystalline polymers this corresponds to the crystalline spacing. There are essentially two SAXS methods for crystallinity determination. The theoretically most precise was developed over a long period (*sic*), and the seminal publications were by Vonk and coworkers[14]. The procedure is based on a one-dimensional semi-crystalline model comprising amorphous and crystalline layers. A correlation function is defined from which the volume fraction of crystals is calculated from the horizontal region in the first minimum. A more robust method[2] involves the calculation of the invariant Q, which is independent of the size and shape of the scattering entities and is a quadratic in the volume fraction of crystals ϕ and a linear function of the electron density difference $\langle \eta^2 \rangle$ between the two phases. The invariant may be calculated from the integral

$$Q = \phi(1-\phi)\langle \eta^2 \rangle = \frac{1}{2\pi i_e} \int_0^\infty I(q) q^2 \, dq \qquad (1)$$

where $I(q)$ is the scattered intensity, q is the scattering vector and i_e is the Thompson scattering factor. If $\langle \eta^2 \rangle$ for the system is known, the quadratic in ϕ may be readily solved. The quantity Q is known as the invariant, being independent of the size and shape of the structural heterogeneities. The invariant passes through a maximum at 50% crystallinity for the two-phase model, and this was pointed out by Strobl and Schnieder[15]. The two-phase model has been expanded to a pseudo-two-phase model by Ruland and coworkers[16] to include a transition layer or interface of smooth electron density between the crystalline and amorphous lamellae. In some cases, where the data are of a very high statistical quality, correlation function analyses can yield further spatial information, such as the thickness of the interface between the crystalline and amorphous regions of a semicrystalline polymer[17].

Conventional SAXS and WAXS experiments, that is those utilizing sealed tube or rotating anode X-ray sources, are limited to stable materials because of the long times (hours) required to obtain patterns of sufficient statistical quality (signal to noise ratio). Patterns may be taken as a function of temperature, but generally this is not done owing to the difficulties of furnace design. The major problem is with leakage after long times at high temperatures and subsequent camera contamination. To obtain statistically significant SAXS and WAXS patterns for the study of crystallization and melting (time resolution of less than 1 min and preferably less than 1 s), a high flux of synchrotron radiation and fast, position-sensitive electronic detectors must be used[18].

Time-resolved synchrotron X-ray studies of polymer crystallization and melting have been pioneered using the combined techniques of d.s.c.–SAXS[19–21] and d.s.c.–WAXS[22] by Koberstein and coworkers. The inevitable conclusion of Koberstein's work is that combined SAXS–WAXS is a step towards minimizing experimental effort and realizing unambiguous results by removing the need for repeated experiments on different samples.

Ungar and Feijoo[23] have also used d.s.c.–SAXS and d.s.c.–WAXS to study chain folding in the crystallization of high-molecular-weight, monodisperse, linear alkanes and the morphological transitions of side-chain liquid crystalline polymers. The need for simultaneous SAXS–WAXS is also borne out by this work.

An ideal simultaneous SAXS–WAXS experiment would provide spatial information over size scales from 1 to 1000 Å, as illustrated in *Figure 1*. The SAXS experiments allow calculation of the lamellar spacing from the peak maximum and calculation of the invariant. The crystal structure can be deduced from the positions of the peaks in the WAXS pattern and the degree of crystallinity can be calculated from the ratios of the intensities. The synergy of the information available from time-resolved SAXS–WAXS has attracted much interest, and three such instruments have been constructred.

At DESY in Germany, Zachman *et al.*[24] made the

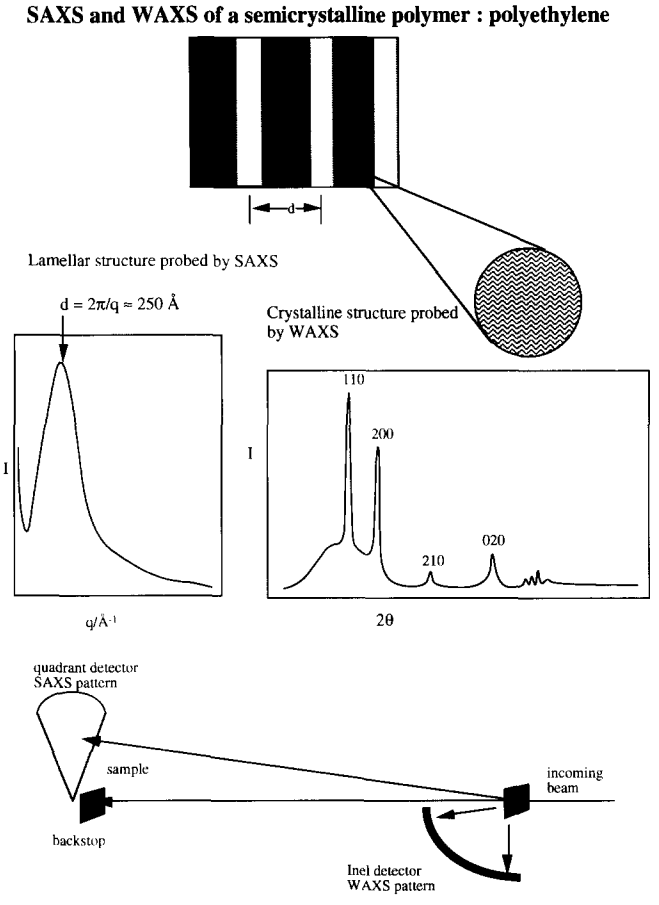

Figure 1 Spatial information available from SAXS and WAXS experiments on semicrystalline polymers. The SAXS experiments allow calculation of the lamellar spacing from the peak maximum. The crystal structure may be deduced from the positions of the peaks in the WAXS pattern. The camera geometry is also shown

first attempt at combining WAXS and SAXS to study poly(ethyleneterephthalate) and its related liquid crystalline polymers. Owing to the experimental arrangement used, the data had a poor signal to noise ratio at d.s.c. heating rates. This pioneering work cannot be ignored; despite the limitations of the signal to noise ratio in calculating phase compositions, good spatial information was obtained.

Chu *et al.*[25] at the NSLS have recently constructed a SAXS–WAXS camera and used it to study the melting and crystallization of polyolefin blends. Although their camera had good spatial resolution in both the small-angle and wide-angle regimes, the angular range for WAXS was limited by the use of a linear detector to $\sim 10^\circ$ of arc and the SAXS camera was compromised by underfocused Kratky optics. The degree of crystallinity was calculated from the ratio of the integrated intensity of the crystal peaks to the integrated intensity over the detector. The relative invariant was calculated from the area under a Lorentz-corrected scattering curve. The time evolutions of the invariant and the degree of crystallinity were discussed but the two were not directly correlated.

At Daresbury we have recently constructed a SAXS–WAXS camera on a high-intensity pinhole optics beamline optimized for isotropic scatterers and equipped with a quadrant detector for SAXS and a curved detector for WAXS that covers $>70^\circ$ of arc[26]. The problems associated with the two previously reported set-ups were mainly alleviated. The experimental set-up has been described in a previous publication[26] and typical data obtained during the melting and crystallization of high-density polyethylene (HDPE) are presented in *Figure 2*. The patterns were collected with a time resolution of 10 s between 100 and 160°C and the experiments are described in detail below. Temperature-dependent WAXS and SAXS patterns from HDPE have appeared before in the literature[2,25–27], and so our primary data form part of the introduction. The SAXS patterns show a strong peak in $I(q)q^2$ (at q^*) which increases in intensity and then collapses towards the beamstop as the polymer melts, while the WAXS data show strong peaks (which have been indexed to the orthorhombic structure) which drop continuously in intensity as the material melts. These patterns are consistent with individual lamellae melting in a first-order thermodynamic process; the degree of crystallinity is falling (WAXS intensities reduce) and the average correlation length increasing (peak moves to lower q^*). The recrystallization processes illustrate the reversibility of the whole process: a weak SAXS peak appears at low q and grows through a maximum in intensity to a constant q^* and the WAXS peaks just grow to a maximum. These patterns are consistent with the sporadic nucleation of lamellae that grow laterally and thicken.

This paper describes a method of assessing the degree of crystallinity and lamellar thickness directly from the data presented in *Figure 2*. The maximum in the invariant at 50% crystallinity will be used to calibrate the integrated intensities from WAXS.

EXPERIMENTAL

Simultaneous SAXS–WAXS measurements were made on beamline 8.2 of the SRS at the SERC Daresbury Laboratory, Warrington, UK. The details of the storage ring, radiation and camera geometry and data collection electronics have been given in detail elsewhere[26]. The camera is equipped with a multiwire quadrant detector (SAXS) located 3.5 m from the sample position and a curved knife-edge detector (WAXS) that covers 120° of arc at a radius of 0.2 m. A vacuum chamber is placed between the sample and detectors in order to reduce air scattering and absorption. Both the exit window of the beamline and the entrance window of the vacuum chamber are made from 15 μm mica; the exit windows of the vacuum chambers are made from 15 μm mica and 10 μm Kapton film for the WAXS and SAXS detectors, respectively. The WAXS detector has a spatial resolution of 50 μm and can handle up to $\sim 150\,000$ counts s^{-1}; only 90° of arc are active in these experiments, the rest of the detector being shielded with lead. A beamstop is mounted just before the SAXS exit window to prevent the direct beam from hitting the SAXS detector, which measures intensity in the radial direction (over an opening angle of 70° and an active length of 0.2 m) and is only suitable for isomorphous scatterers. It has an advantage over single-wire detectors in that the active area increases radially, improving the signal to noise ratio at larger scattering angles. The spatial resolution of the SAXS detector is 400 μm and it can handle up to $\sim 500\,000$ counts s^{-1}.

The specimens for SAXS–WAXS were prepared by placing an HDPE disc ~ 0.5 mm thick and ~ 8 mm in diameter, cut from premoulded sheet, in a cell comprising

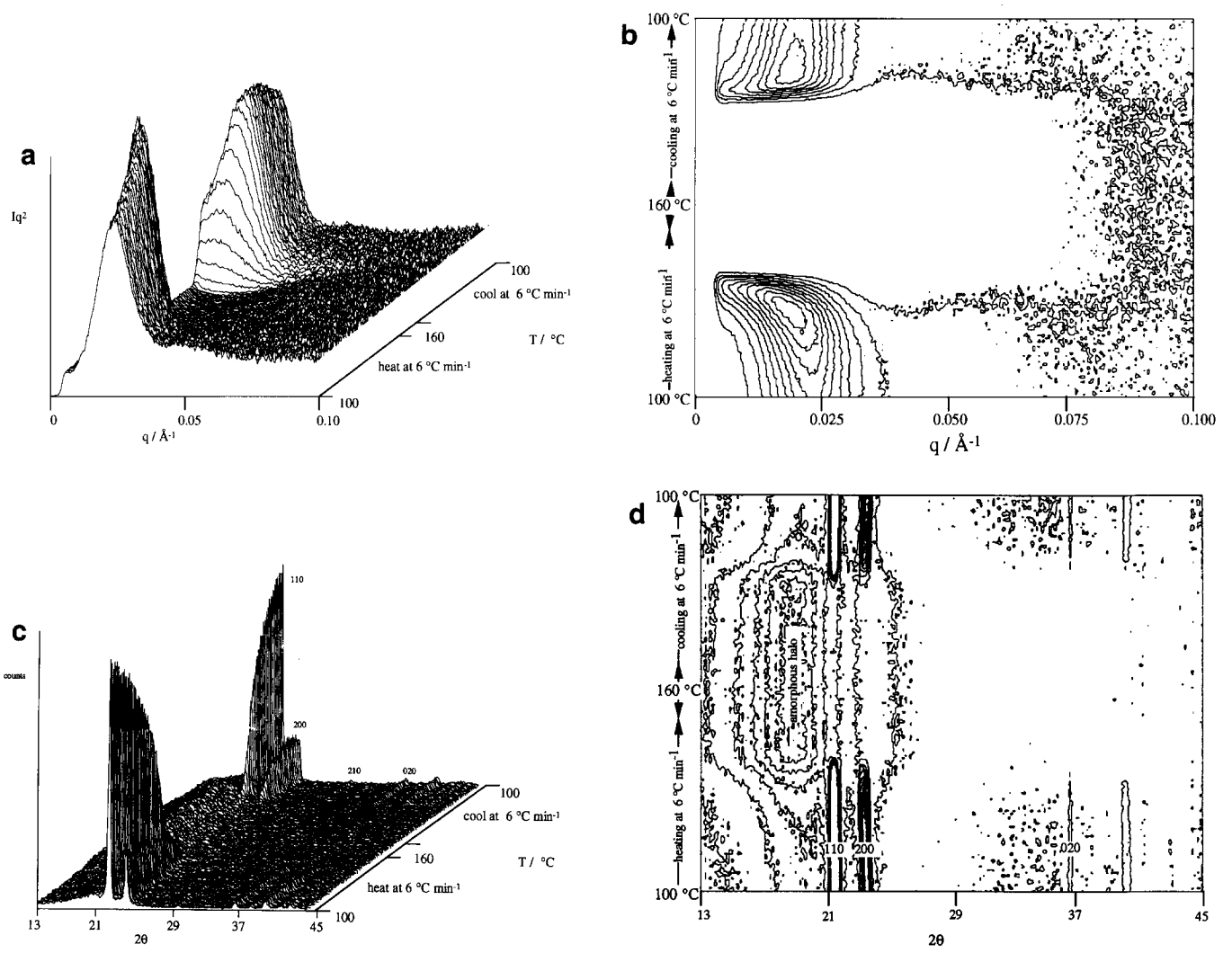

Figure 2 Three-dimensional relief diagrams and the corresponding contour plots of time-resolved SAXS and WAXS data obtained with a time resolution of 10 s during melting and recrystallization of high-density polyethylene at a ramp rate of 6°C min^{-1}. For ease of interpretation the time axis has been transformed into temperature. (a) Three-dimensional plot of Lorentz-corrected SAXS intensity $I(q, t)q^2$ *versus* the scattering vector q *versus* temperature T. (b) SAXS contour plots with isointensity contours for the Lorentz-corrected intensity $I(q, t)q^2$ *versus* the scattering vector q *versus* temperature T. (c) Three-dimensional plot of WAXS intensity $I(2\theta, t)$ *versus* the scattering angle 2θ *versus* temperature T. (d) WAXS contour plots with isointensity contours for the scattered intensity $I(2\theta, t)$ *versus* the scattering angle 2θ *versus* temperature T

a Du Pont d.s.c. pan fitted with windows (~7 mm in diameter) made from 5 μm thick mica. The modified d.s.c. pans are described elsewhere[20,28]. Loaded, sealed pans were glued to a J-type thermocouple and placed in a spring-loaded holder in a modified Linkam TMH600 hot stage mounted on the optical bench. The silver heating block of the hot stage contains a 4 × 1 mm conical hole which allows the incident X-rays to pass through unhindered. A nominal heating rate of 10°C min^{-1} was used. Owing to the nature of the furnace, there was a small temperature drift across the sample chamber which required direct measurement of the temperature at the sample position over and above the temperature monitoring and control of the furnace.

The scattering pattern from an oriented specimen of wet collagen (rat-rail tenson) was used to calibrate the SAXS detector and HDPE, aluminium and an NBS silicon standard were used to calibrate the WAXS detector. A parallel plate ionization detector placed before the sample cell recorded the incident intensity. The experimental data were corrected for background scattering (subtraction of the scattering from the camera, hot stage and an empty cell), sample thickness and transmission and the positional non-linearity of the detectors.

DATA ANALYSIS

SAXS data analysis

A peak or a shoulder in $I(q)$ gives a general indication of the presence of a periodic structure in the system. The most common practice for determining the periodicity is to use Bragg's law in the calculation of a domain spacing d from the location of the peak maximum q_{max} in an intensity *versus* scattering vector plot

$$d = \lambda/2 \sin \theta_{max} = 2\pi/q_{max} \quad (2)$$

The peak in the bare intensity data in *Figure 3* is weak, making unambiguous determination of q_{max} difficult if not impossible. For the polymers in the present study, more precise information regarding microstructural periodicity is obtained if the morphology is assumed to be globally isotropic but locally lamellar[3]. The data can then be analysed to give a one-dimensional Bragg spacing d_1 by applying the Lorentz correction q^2 to the observed scattered intensity $I(q)$. *Figure 3* shows a plot of $I(q)q^2$

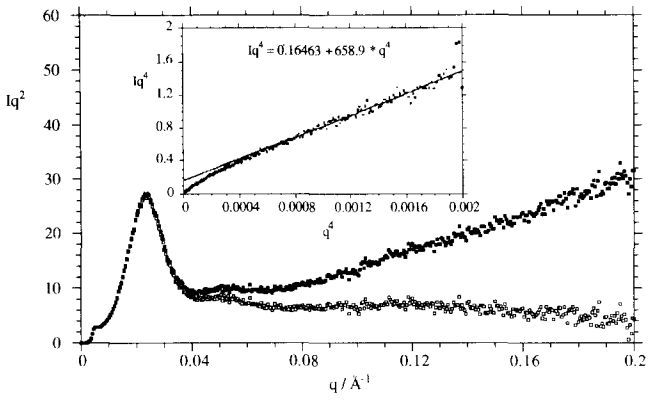

Figure 3 Lorentz-corrected SAXS patterns at 100°C. The effects of diffuse scattering from the thermal background at high q are obvious in the raw data $I(q)q^2$ *versus* q (■) and their corrected values $[I(q)-I_b]q^2$ *versus* q (□). The inset is the Porod plot used to calculate the thermal background from the slope of the linear portion in $I(q)q^4$ *versus* q^4

versus q for high-density polyethylene at 100°C. For materials with sharp phase boundaries, Porod's law[29] predicts a fall off in q^{-4} for scattered intensity at large angles

$$\lim_{q\to\infty} I(q) = (K_p/q^4) + I_b \tag{3}$$

The quantity I_b arises from density fluctuations and K_p is the Porod constant. Note the strong positive deviation in the Porod plot ($I(q)q^4$ *versus* q^4) illustrated as an inset to *Figure 3*. Positive deviations from Porod's law are caused by thermal density fluctuations[12]. A regression analysis of the linear part of the curve gives values of $K_p = 0.164$ and $I_b = 659$. I_b must be subtracted from the raw intensity data before both d_1 and the invariant are calculated.

The open symbols in *Figure 3* are values of $I'q^2$ ($=[I(q)-I_b]q^2$) *versus* q and the artificial upturn of $I(q)q^2$ at high q has been corrected (filled symbols). The first-order reflection is very strong and a second-order reflection may also be observed, indicating that the interface between crystalline and amorphous regions is sharp and a two-phase model is appropriate[27]. For the calculation of the Bragg spacing, the maximum in $I'q^2$ *versus* q is taken as q^*, so that $d_1 = 2\pi/q^*$. The peak value at 100°C from $I(q)$ *versus* q gives a d spacing of ~330 Å, whereas the peak value from $I'q^2$ *versus* q gives a d_1 spacing of 273 Å. The fully corrected d_1 spacing will be used in the discussion.

The invariant Q, which is linear in the electron density difference $\langle\eta^2\rangle$ between the crystalline and amorphous phases and quadratic in the volume fraction of crystals ϕ, may be obtained from the integral in equation (1). The absolute value of the invariant requires absolute intensity measurements, thermal background subtraction and extrapolation to $q=0$ and ∞, and is computationally difficult to achieve. The major contribution to the experimental invariant can be used to characterize structure development, as well as the degree of microphase separation, and is readily assessed by a Simpson's rule integration of the $I(q)q^2$ *versus* q curve between the experimental limits[17]. A relative invariant Q' has been calculated by summation of the area under the $I'q^2$ *versus* q curve between the first reliable data point, $q = 0.01$ Å^{-1}, and the region in which $I(q)q^2$ becomes constant, i.e. at $q = 0.20$ Å^{-1}, according to

$$Q' = \int_{0.01}^{0.20} [I(q) - I_b]q^2 \, dq \tag{4}$$

Owing to the relative nature of the intensity measurement, the value of Q' is also only relative with arbitrary units. The Lorentz-corrected SAXS patterns in *Figure 4* are those used to obtain the relative invariant and illustrate how the peak position shifts to lower q (larger d spacings) and the peak intensity initially increases then decreases as the invariant passes through a maximum. This feature is used in the calculation of $\phi = 0.5$ in order to calibrate the WAXS-integrated intensity.

WAXS data analysis

The WAXS patterns in *Figures 2c* and *2d* have been corrected for the detector response function and changes in sample thickness during the experiment but have not been corrected for the change in absorbance caused by path length changes when performing WAXS experiments in transmission. The patterns have been indexed according to the literature[3]. *Figure 5* illustrates the temperature sensitivity of the 110 and 200 lattice reflections in terms of the peak position and intensity between 100 and 160°C. The increased lattice expansion of the 200 compared to the 110 is well established[2,3,25]. There are two types of measurement for the degree of crystallinity by WAXS. External comparison methods are those involving the comparison of an experimental WAXS pattern with patterns of wholly crystalline and wholly amorphous standards. Internal comparison methods are those which use the integrated intensities of the patterns associated with the amorphous and crystalline features. To a first approximation, the degree

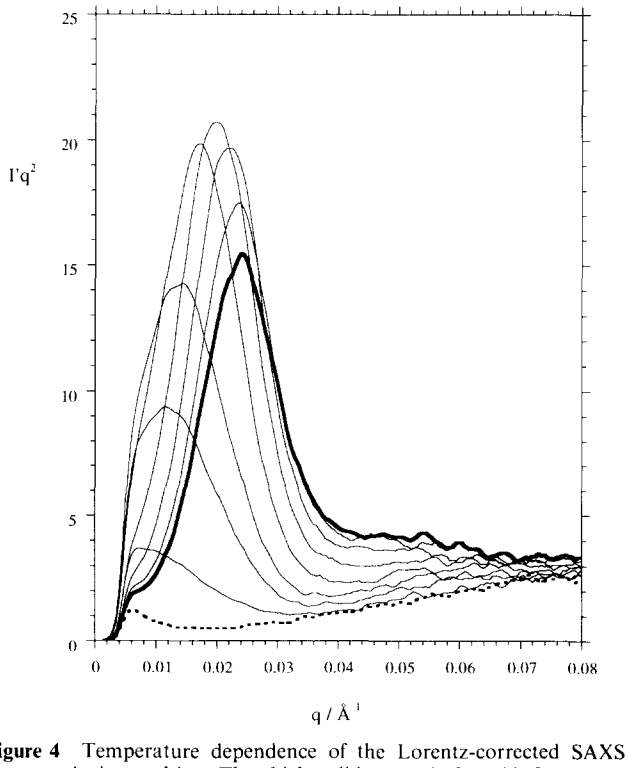

Figure 4 Temperature dependence of the Lorentz-corrected SAXS patterns during melting. The thick solid curve is for 100 C and the thick dashed curve is for 160 C. The peak position moves towards lower q as the temperature increases

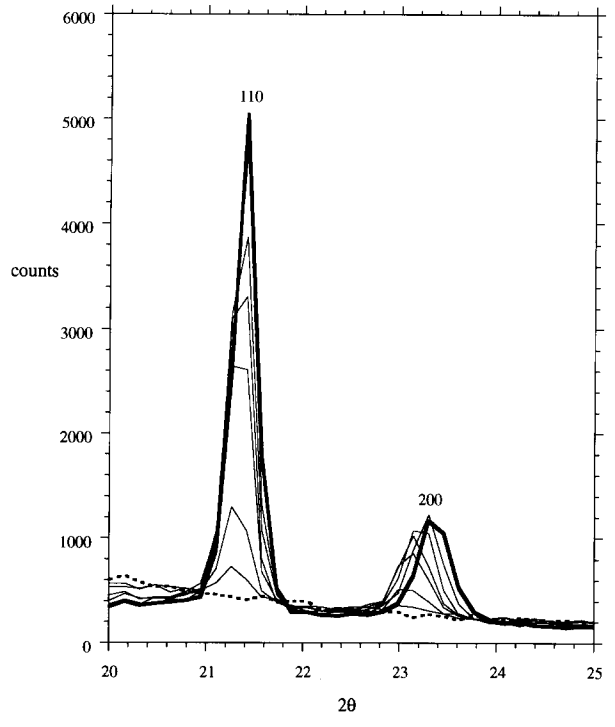

Figure 5 Temperature dependence of the 110 and 200 regions of the WAXS patterns during melting. The thick solid curve is for 100°C and the thick dashed curve is for 160°C. The 200 peak position moves to lower 2θ as the temperature increases

of crystallinity can be obtained by assuming that the total scattering within a certain region of reciprocal space is independent of the state of aggregation of the polymer. The degree of crystallinity (mass fraction) may then be found from

$$X_c = I_c/I_t \tag{5}$$

where I_c is the contribution of the crystalline component to the total scattering $I_t = I_c + I_a$. An example of this simple type of calculation for polyethylene is given in the introductory polymer textbook of Young and Lovell[30] as being the ratio of the areas under the 110 and 200 peaks, viz.

$$X_c = A_c/(A_c + A_a) \tag{6}$$

where A_a is the area under the amorphous peaks and A_c is the area remaining under the crystalline peaks. The area under the strongest reflection, the 110, has been calculated by Simpson's rule integration between the limits $20.9 < 2\theta < 21.9$ as a first-order approximation to the degree of crystallinity. We use a simple integration for WAXS because the peak lineshape is somewhat instrument resolution limited and, as such, any fitting routine will be a complex function of both the instrument resolution and the intensity. The integrated intensity at $T \gg T_m$ gives the value of I_a and the integrated intensity at $T < T_m$ gives the value of $I_t = I_c + I_a$, allowing I_c to be calculated. Without performing numerical analysis on the whole pattern or in the absence of any method of calibration, the integrated intensity of a single reflection may only be used to get semiquantitative information on the degree of crystallinity. The magnitude of I_c when $X_c = 0$ ($T \gg T_m$) is known and the magnitude of I_c when X_c is a maximum is known, but unless there is external calibration of the maximum in X_c the measurements are arbitrary and qualitative.

Internal calibration by simultaneous SAXS–WAXS

The relative invariant Q' from SAXS and the integrated intensity I_{110} from WAXS are plotted as a function of time (during a heating and cooling experiment) in *Figure 6*. In the first 600 s of heating the value of I_{110} falls continuously from 130 ± 3 to a constant 50 ± 2, whereas Q' initially increases from 1250 ± 10 to a maximum of 1330 ± 10 before falling to a constant value of 522 ± 7. The constant values at 600 s ($T = 160$°C) are those of the amorphous molten polymer. The maximum in Q' comes from the relationship

$$Q' = \phi(1-\phi)\langle\eta^2\rangle \tag{7}$$

which is linear in the electron density difference $\langle\eta^2\rangle$ and quadratic in the volume fraction ϕ of crystals[3,15,27]. If we assume that the two-phase model[14] applies and $\langle\eta^2\rangle$ is a constant, then the invariant passes through a maximum[15] at $\phi = 0.5$. This assumption allows two important further procedures. Firstly, the value of I_{110} when Q' is a maximum (I_{Q^*}) may be interpreted as being that where the volume fraction of crystals $\phi = 0.5$. The relationship between the volume and mass fractions of crystals is simply

$$X_c = \phi\rho_c/\rho \tag{8}$$

where ρ_c is the density of the pure crystal and ρ is the density of the semicrystalline polymer. Therefore two points on the linear scale $X_c = \phi\rho_c/\rho = I_c/I_t$ are known for $\phi = 0$ and $\phi = 0.5$ in the limit that the semicrystalline polymer density varies linearly between 0.93 at 100°C and 0.85 at the melting point[31]. Secondly, the quadratic may be solved using the value of Q' and $\phi = 0.5$ to give an electron density at that temperature of 328.75 arbitrary units. The electron density difference is also temperature dependent, but this is small compared with the changes in ϕ. Solution of the quadratic for Q' gives two sets of solutions in ϕ which may be compared with the result calculated from I_{110} so that the most reasonable values are taken.

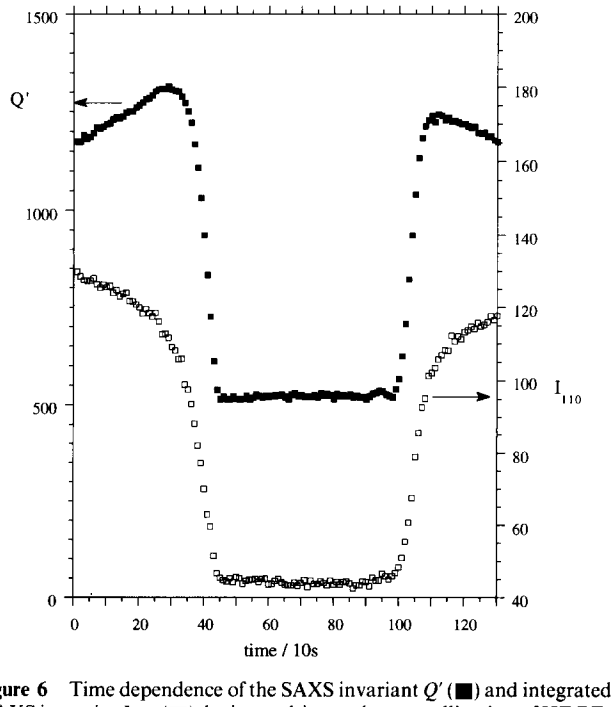

Figure 6 Time dependence of the SAXS invariant Q' (■) and integrated WAXS intensity I_{110} (□) during melting and recrystallization of HDPE

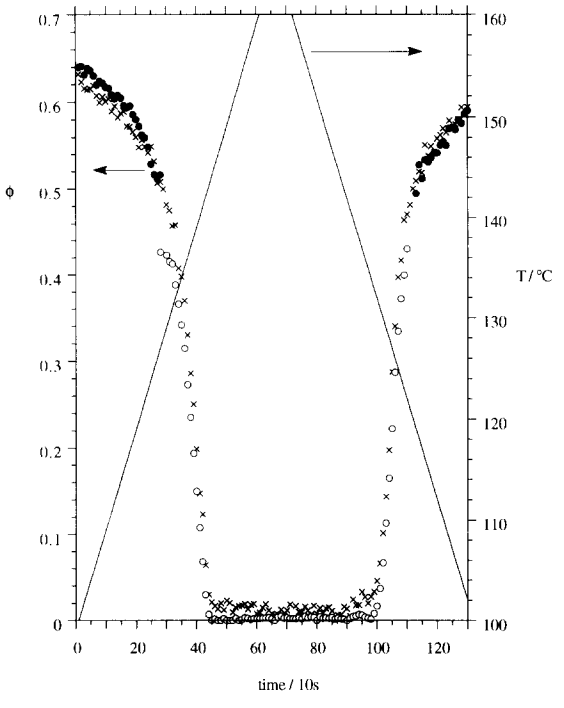

Figure 7 Temperature (——) and the degree of crystallinity ϕ calculated from the integrated WAXS intensity (×) and from the SAXS invariant (○, ●) as a function of time during melting and recrystallization of HDPE. The ϕ from WAXS is calibrated from the integrated intensity across the 110 peak, the associated maximum in Q' being 50% crystallinity[15] and its value at $T=160$ C being zero crystallinity. The ϕ from SAXS is calculated by solving the quadratic in Q' and correcting for changes in density

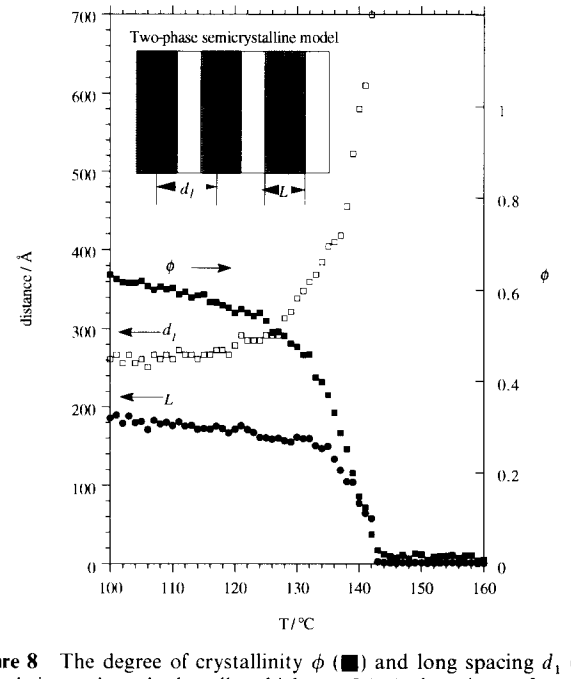

Figure 8 The degree of crystallinity ϕ (■) and long spacing d_1 (□) with their product the lamellar thickness L(●) plotted as a function of temperature. The relationship between the parameters is illustrated by the two-phase semicrystalline model, which is included as an inset

The values of ϕ are calculated from the WAXS data using

$$\phi(\text{WAXS}) = I - I_a / 2(I_{Q^*} - I_a) \quad (9)$$

and values of ϕ calculated from the quadratic equation of the invariant, corrected for the linear change in the (electron) density difference[27], are plotted against time in *Figure 7*. The crosses are the WAXS data and the circles are the SAXS data (filled and open circles being the two sets of solutions). The correlation between the degree of crystallinity from WAXS and the degree of crystallinity from SAXS is good considering the assumptions made in the calculation.

Calculation of the lamellar thickness L *from the degree of crystallinity and long spacing*

In the two-phase model the average lamellar thickness L is given by the product of the degree of crystallinity ϕ and the long spacing d_1. *Figure 8* is a plot of the measured parameters ϕ and d_1 and the calculated value of L according to the two-phase model (which is included as an inset)[2,3,15]. The degree of crystallinity falls and the long spacing increases with temperature as one would expect; individual lamellae melt out in a first-order fashion, the lower-order lamellae melting at lower temperatures. The average lamellar thickness remains constant prior to falling asymptotically at the melting point. This is counter intuitive as the thinnest lamellae (those having the greatest interfacial area) should melt first, causing the d spacing to increase[1,3,14]. The experimental result can be rationalized, however, by considering a growing interface causing an apparent reduction in ϕ.

SUMMARY AND CONCLUSIONS

A newly constructed camera at the SRS, Daresbury has been used to assess the degree of crystallinity and lamellar thickness of HDPE from simultaneously obtained SAXS and WAXS patterns during melting and crystallization. The long spacing was obtained, in the conventional manner, from the peak in the Lorentz-corrected SAXS pattern. The degree of crystallinity was obtained from a combination of the SAXS invariant and the integrated WAXS intensity of the crystals. The invariant passes through a maximum at 50% crystallinity[15,27] and the integrated WAXS intensity is a minimum for the melt. The maximum in Q' calibrates the corresponding I_{110} to be that for $\phi=0.5$, the melt value of I_{110} corresponding to $\phi=0$; thus, two points in the linear relationship between the WAXS intensity and the degree of crystallinity are known. Calculation of the crystallinity by solving the quadratic of ϕ in Q' gives good agreement with the WAXS result once the changes in density have been taken into account. The long spacing and the degree of crystallinity may be combined in the two-phase model to estimate the lamellar thickness. The melting process is characterized by a gradual reduction in the degree of crystallinity and an increase in the long spacing, and this is because of the first-order melting of low-order crystals. These two effects combine to give a lamellar spacing that does not appear to change during the melting process, which is counterintuitive[3].

ACKNOWLEDGEMENTS

These experiments would have been impossible without the support of Neville Greaves, Jim Sheldon, Dave Bouch, Paul Hindley and Brian Parker. Constructive criticism of the manuscript by Rob Rule and William O'Kane is gratefully acknowledged.

REFERENCES

1 Mandelkern, L. in 'Comprehensive Polymer Science' (Eds G. Allen and J. C. Bevington), Vol. 1, Pergamon Press, Oxford, 1988, p. 363
2 Sperling, L. H. 'Introduction to Physical Polymer Science', John Wiley & Sons, New York, 1986
3 Baltá-Calleja, F. J. and Vonk, C. 'X-ray Scattering of Polymers', Elsevier, Amsterdam, 1989
4 Nakamura, N. K. *J. Appl. Polym. Sci.* 973, **17**, 1031
5 Keonig, J. L. 'Spectroscopy of Polymers', ACS, Washington, DC, 1991
6 Cullity, D. B. 'Elements of X-ray Diffraction', Addison-Wesley, Reading, MA, 1978
7 Goppel, J. M. and Arlman, J. J. *Appl. Sci. Res. A* 1949, **1**, 462
8 Statton, W. O. *J. Appl. Polym. Sci.* 1963, **7**, 803
9 Wakelin, J. M. and Young, J. *J. Appl. Polym. Sci.* 1966, **10**, 1421
10 Ruland, W. *Acta Crystallogr.* 1961, **14**, 1180
11 Hindleh, A. M. and Johnson, D. J. *J. Phys.* 1971, **4**, 259
12 Vonk, C. G. *J. Appl. Crystallogr.* 1973, **6**, 148
13 Rabiej, S. and Wlochowicz, A. *Angew. Makromol. Chem.* 1990, **175**, 81
14 Vonk, C. G. *J. Appl. Crystallogr.* 1975, **8**, 340
15 Strobl, G. R. and Schnieder, M. J. *J. Polym. Sci., Polym. Phys. Edn* 1981, **19**, 1361
16 Ruland, W. *J. Appl. Crystallogr.* 1971, **4**, 70
17 Vonk, C. G. *J. Appl. Crystallogr.* 1973, **6**, 81
18 Catlow, C. R. A. and Greaves, G. N. 'Applications of Synchrotron Radiation', Blackie, Glasgow, 1980
19 Koberstein, J. T. and Russell, T. P. *J. Polym. Sci., Polym. Phys. Edn* 1985, **23**, 1109
20 Koberstein, J. T. and Russell, T. P. *Macromolecules* 1986, **19**, 714
21 Koberstein, J. T., Yu, C. C., Galambos, A. F., Russell, T. P. and Ryan, A. J. *Polym. Prepr. Am. Chem. Soc. Div. Polym. Chem.* 1990, **31**, 110
22 Koberstein, J. T. and Galambos, A. F. *Macromolecules* 1992, **25**, 5618
23 Ungar, G. and Feijoo, J. L. *Mol. Cryst. Liq. Cryst. B* 1990, **180**, 281
24 Bark, M., Schulze, C. and Zachmann, H. G. *Polym. Prepr. Am. Chem. Soc. Div. Polym. Chem.* 1990, **31**, 163
25 Tashiro, K., Satkowski, M. M., Stein, R. S., Li, Y., Chu, B. and Hsu, S. L. *Macromolecules* 1992, **25**, 1809
26 Bras, W., Derbyshire, G. E., Ryan, A. J., Mant, G. R., Felton, A., Lewis, R. A., Hall, C. J. and Greaves, G. N. *Nucl. Instrum. Meth. Phys. Res. A* 1993, **326**, 587
27 Schoeterden, P., Vandermarliere, M., Reikel, C., Koch, M. H. J., Groeninckx, G. and Reynaers, H. *Macromolecules* 1989, **22**, 237
28 Ryan, A. J. *J. Therm. Anal.* 1993, **40**, 887
29 Porod, G. *Kolloid Z. Z. Polym.* 1951, **124**, 83
30 Young, R. J. and Lovell, P. A. 'Introduction to Polymers', Chapman and Hall, London, 1991
31 van Krevelen, D. W. 'Properties of Polymers: Correlations with Chemical Structure', 3rd Edn, Elsevier, Amsterdam, 1991